Cancer Cell
Article

The *DLEU2/miR-15a/16-1* Cluster Controls B Cell Proliferation and Its Deletion Leads to Chronic Lymphocytic Leukemia

Ulf Klein,[1,6] Marie Lia,[1] Marta Crespo,[1] Rachael Siegel,[1,7] Qiong Shen,[1] Tongwei Mo,[1] Alberto Ambesi-Impiombato,[2] Andrea Califano,[1,2] Anna Migliazza,[1,5] Govind Bhagat,[1,3] and Riccardo Dalla-Favera[1,3,4,*]
[1]Institute for Cancer Genetics and the Herbert Irving Comprehensive Cancer Center
[2]Joint Centers for Systems Biology
[3]Department of Pathology & Cell Biology
[4]Department of Genetics & Development
Columbia University, New York, NY 10032, USA
[5]Nerviano Medical Sciences, viale Pasteur 10, 20014 Nerviano, Milano, Italy
[6]Present address: Herbert Irving Comprehensive Cancer Center, Department of Pathology & Cell Biology and Departments of Microbiology & Immunology, Columbia University, New York, NY 10032, USA
[7]Present address: HUMIGEN, the Institute for Genetic Immunology, Hamilton, NJ 08690, USA
*Correspondence: rd10@columbia.edu
DOI 10.1016/j.ccr.2009.11.019

SUMMARY

Chronic lymphocytic leukemia (CLL) is a malignancy of B cells of unknown etiology. Deletions of the chromosomal region 13q14 are commonly associated with CLL, with monoclonal B cell lymphocytosis (MBL), which occasionally precedes CLL, and with aggressive lymphoma, suggesting that this region contains a tumor-suppressor gene. Here, we demonstrate that deletion in mice of the 13q14-minimal deleted region (MDR), which encodes the *DLEU2/miR-15a/16-1* cluster, causes development of indolent B cell-autonomous, clonal lymphoproliferative disorders, recapitulating the spectrum of CLL-associated phenotypes observed in humans. miR-15a/16-1-deletion accelerates the proliferation of both human and mouse B cells by modulating the expression of genes controlling cell-cycle progression. These results define the role of 13q14 deletions in the pathogenesis of CLL.

INTRODUCTION

B cell chronic lymphocytic leukemia (CLL) represents the most common B cell-derived malignancy of adults with an incidence of around 1 in 100,000 per year. The disease is characterized by the clonal expansion of B cells that express the CD5 cell surface antigen and that are thought to derive from antigen-experienced marginal zone B cells (Chiorazzi and Ferrarini, 2003; Klein et al., 2001). Within this morphologically homogeneous tumor, two subtypes of CLL have been identified: one that expresses somatically mutated immunoglobulin variable region (IgV) genes and has a good prognosis, and one with unmutated IgV genes and a less favorable prognosis (Chiorazzi and Ferrarini, 2003; Damle et al., 1999; Hamblin et al., 1999). Recent work suggests that CLL may be preceded by $CD5^+$ monoclonal B cell lymphocytosis (MBL), which is detectable in ~5% of the healthy elderly population and that can progress to CLL in ~1% of cases (Landgren et al., 2009; Rawstron et al., 2008). A small fraction of CLL progresses toward a more aggressive malignancy diagnosed as diffuse large B cell lymphoma (DLBCL).

The pathogenesis of CLL remains obscure because no genetic alteration has been conclusively demonstrated to contribute to its pathogenesis. Although CLL only rarely shows reciprocal

SIGNIFICANCE

Emerging evidence has suggested the presence of a tumor-suppressor locus in the chromosomal region 13q14 commonly deleted in CLL. These results show that this region has a major role in controlling the pool of mature B-lymphocytes in vivo. Its deletion causes a heterogeneous B-cell-autonomous phenotype that recapitulates the spectrum of CLL-associated syndromes including MBL and lymphoma. Within the 13q14-region, the *miR-15a/16-1* cluster plays a role in controlling the proliferation of B cells, but additional genetic elements invariably deleted in human CLL contribute to the aggressiveness of the phenotype. These results elucidate the mechanism by which miR-15a/16-1 function in vivo, provide a faithful mouse model of human CLL, and provide a paradigm for the tumor-suppressor role of sterile RNA transcripts.

balanced chromosomal translocations (Döhner et al., 2000; Mayr et al., 2006), the spectrum of genomic aberrations in CLL includes trisomy of chromosome 12 (16%) and deletion of chromosomal regions 17p (p53; 7%), 11q (18%), and 13q14.3 (further on designated as 13q14), which represents the most common genomic aberration in CLL (55%) (Döhner et al., 2000; Kalachikov et al., 1997). Inactivation of p53 is observed in a fraction of cases and is associated with disease progression (Gaidano et al., 1991).

Deletion of 13q14 is mostly monoallelic (76% of cases), but can be biallelic (24%) (Döhner et al., 2000). This deletion occurs in CLL with somatically mutated as well as unmutated IgV genes, although it is more prevalent in the former subtype (~80% versus 20%). 13q14 deletions are found at high frequency (>50%) also in MBL (Rawstron et al., 2008) and at lower frequency in CD5-negative B cell-derived malignancies (Avet-Loiseau et al., 1999; Cigudosa et al., 1998; Liu et al., 1995; Stilgenbauer et al., 1998), including DLBCL and multiple myeloma, as well as mature T cell lymphomas (Rosenwald et al., 1999), and in a variety of solid tumors.

Because 13q14 deletions suggest the presence of a tumor-suppressor gene, this region has been extensively characterized (Bullrich et al., 2001; Corcoran et al., 1998; Liu et al., 1997; Migliazza et al., 2001; Rondeau et al., 2001; Stilgenbauer et al., 1998). A minimal deleted region (MDR) has been identified (Liu et al., 1997; Migliazza et al., 2001) that comprises the *deleted in leukemia* (*DLEU*) *2* gene, encoding a sterile transcript, parts of the *DLEU1* (1st exon) sterile gene, as well as the microRNA (miR)-15a/16-1 cluster (Calin et al., 2002; Lagos-Quintana et al., 2001) that is located intronic to *DLEU2* (see Figure 1A). Although *DLEU2* and the *miRs* are evolutionary conserved and expressed in B cells (Cimmino et al., 2005; Mertens et al., 2002; Migliazza et al., 2001), a role of *DLEU1* as well as the adjacent *DLEU5* and *KCNRG* genes (Ivanov et al., 2003) in CLL pathogenesis is considered unlikely based on lack of evolutionary conservation (*DLEU1*), inclusion in only a subset of 13q14 deletions (*DLEU5*, *KCNRG*), and low to absent expression in mature B cells (*KCNRG*). Taken together, these observations pointed toward *DLEU2* and/or *miR-15a/16-1* as the candidate tumor suppressors targeted by 13q14 deletions in CLL.

DLEU2 encodes a long noncoding RNA (1.0–1.8 kb) that is polyadenylated and spliced (Migliazza et al., 2001). Members of this class of sterile RNAs exert diverse cellular functions including X chromosome inactivation or activation, imprinting, and transcriptional coactivation or regulation of gene expression (Ponting et al., 2009). The function of DLEU2, however, is unknown, and its sequence does not display homology to any other noncoding RNA. A role for miR-15a/16-1 in CLL pathogenesis has been repeatedly proposed based on in vitro studies in nonlymphoid cell systems that suggested functions of miR-15a/16-1 in negative regulation of proliferation and apoptosis (Bandi et al., 2009; Calin et al., 2008; Cimmino et al., 2005; Linsley et al., 2007; Liu et al., 2008; Raveche et al., 2007). Also, CLL cases were identified (2%) that showed germline mutations in the primary precursor of miR-15a/16-1 that appear to affect its processing (Calin et al., 2005), and a point mutation occurring in the 3′ flanking region of *miR-16-1* in NZB mice has been associated with reduced miR-16-1 expression (Raveche et al., 2007). Downregulation of miR-15a/16-1 has also been implicated in the pathogenesis of prostate carcinoma (Bonci et al., 2008). Based on these observations, the *miR-15a/16-1* cluster has been suggested as the culprit of the deletion in CLL, but no formal proof has been obtained.

In order to identify the genetic elements targeted by the putative 13q14 tumor suppressor and to determine their contribution to CLL pathogenesis, we generated transgenic mice that carried conditional alleles that either mimicked the deletion of the *MDR* or that specifically deleted the *miR-15a/16-1* cluster without affecting the expression of DLEU2.

RESULTS

Construction of Mice Deleting the *MDR* or *miR-15a/16-1*

The 13q14 region is conserved on mouse chromosomal region 14qC3 (Figure 1A). In contrast to the human genome, *Kcnrg* and *dLeu5* are intronic of and overlap with *dLeu2*, respectively, although rare splice forms have been described for *DLEU2* in the human that also overlap with those genes (Baranova et al., 2003). Analogous to the human genome, the *miR-15a/16-1* cluster is located intronic of the *dLeu2* gene ~300 bp downstream of exon 4 (Figure 1A bottom). To investigate the consequences of the deletion of the genes encoded within the 13q14 *MDR*, we generated conditional mouse alleles that upon Cre- or Flpe-mediated deletion either mimic the human *MDR* and delete both *dLeu2* and *miR-15a/16-1* (further on referred to as conditional *MDR* allele), or the *miR-15a/16-1* cluster only.

To generate the conditional *MDR* allele, we inserted two *lox*P as well as two *frt* sites in consecutive ES cell targetings into transcriptionally silent regions that are located 110 kb apart (Figure 1B; for details of the targeting, see Figures S1A1 and S1A2, available online) with the 5′ site located approximately 20 kb centromeric to *dLeu5*, and the 3′ site about 5 kb telomeric to the alternative exon 1 (exon 1b) of *dLeu2*. To allow screening for ES cell clones where both targetings occurred on the same chromosome, an eGFP mini gene and a PGK promoter were placed in the centromeric and telomeric targeting vectors, respectively, thus enabling eGFP expression upon Adeno-Cre-mediated deletion of the *lox*P-flanked *MDR*. Correct homologous recombination of the individual targetings and correct Cre-mediated deletion of the *lox*P-flanked region were confirmed by Southern blot analysis (Figure S1A4 and Figure 1B, lower right). Mice carrying the $MDR^{loxP\text{-}frt/+}$ allele were bred with *Flp*-transgenic mice, and the deletion of the *frt*-flanked region was confirmed by Southern blotting (Figure S1A3 and Figure 1B lower left); these mice are further on referred to as $MDR^{+/-}$ mice.

The conditional *miR-15a/16-1* allele was generated by placing the first *lox*P-site centromeric to the *miR-15a/16-1* cluster and the second one within the ~400 bp region that separates the *miR* cluster and exon 4 of *dLeu2* (Figure 1C; for details of the targeting see Figure S1B1). Correct homologous recombination was confirmed by Southern blot analysis (Figure S1B1). The *neo*-resistance marker was deleted by crossing mice with the targeted allele to *Flp*-transgenic mice, further on designated as $miR\text{-}15a/16\text{-}1^{fl/+}$ (conditional) mice (Figure S1B2). Mice carrying the conditional allele were bred with *Cre*-transgenic mice, and deletion of the *lox*P-flanked region was confirmed by Southern blot (Figure 1C and Figure S1B2); these mice are further on

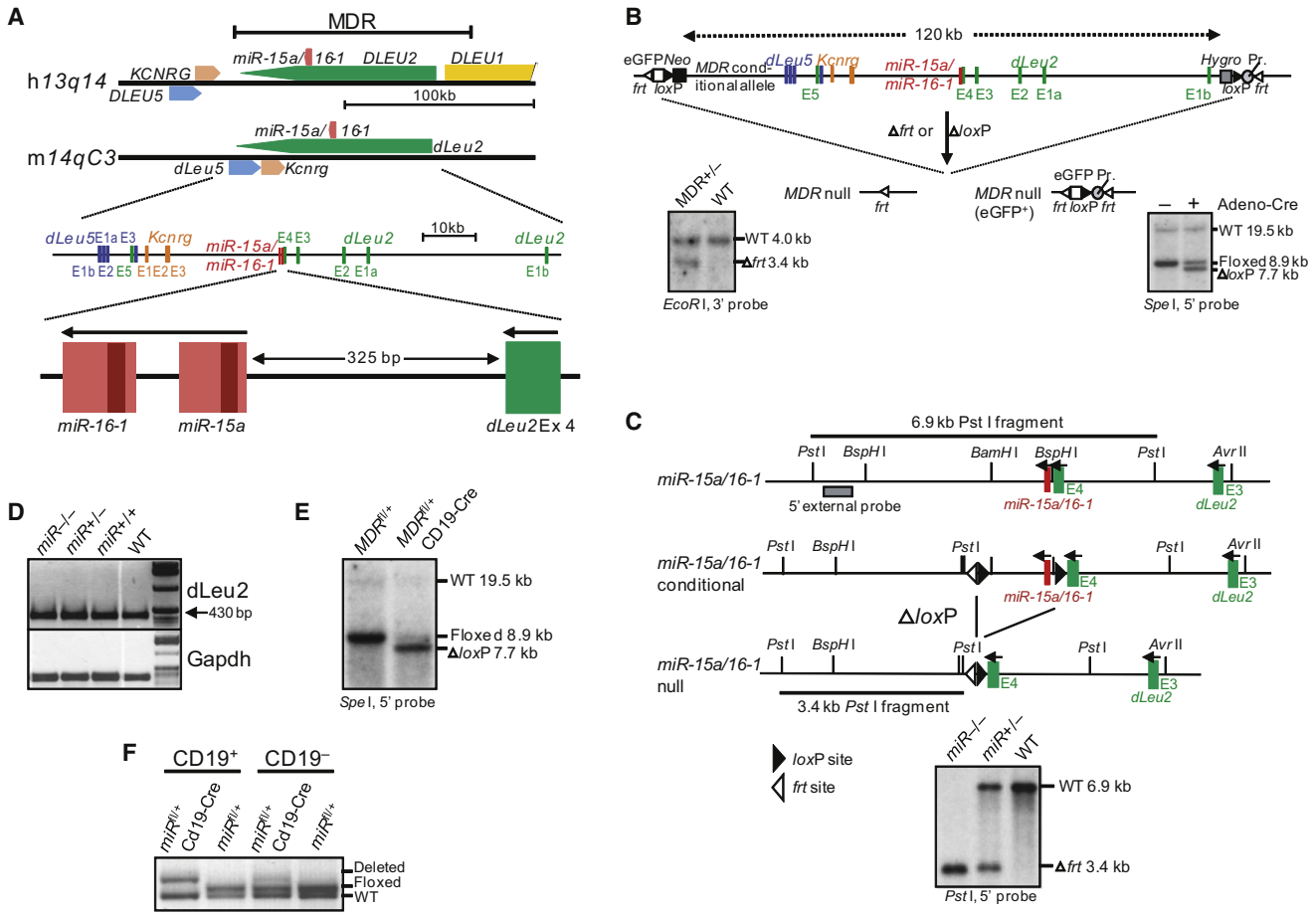

Figure 1. Deletion of the 13q14-*MDR* and of *miR-15a/16-1* in Mice

(A) Schematic representation of the human 13q14 and mouse 14qC3 locus. Genes and their 5′-3′ orientation are indicated by thick arrows. *MDR*, minimal deleted region.

(B) Schematic representation of the *MDR* targeting strategy; for details, see Figures S1A1–S1A4. Indicated are the expected fragments detected by Southern blot analysis after (bottom left) Flp-mediated recombination in mice which generates an *MDR* null allele, and after (bottom right) Adeno-Cre-mediated recombination in $MDR^{fl/+}$ embryonic stem cells (ESCs), which shows a Δ*lox*P fragment besides the targeted fragment, demonstrating the feasibility of deleting the 120 kb conditional *MDR* allele.

(C) Schematic representation of the *miR-15a/16-1* targeting strategy. Correct deletion of *miR-15a/16-1* was identified by Southern blot analysis of PstI-digested DNA that displayed the 3.5 kB deleted band along with the 6.9 kB wild-type (WT) band (right) as indicated in the targeting strategy. For details, see Figure S1B1 and S1B2.

(D) dLeu2 mRNA is normally expressed in *miR-15a/16-1*$^{-/-}$ B cells. RT-PCR from purified $CD19^+$ B cells with oligonucleotides hybridizing in exon 2 (forward primer) and exon 5 (reverse primer) of *dLeu2* showed the expected 430 bp band in all genotypes, demonstrating that the deletion of the *miR-15a/16-1* cluster localized in intron 4 of the *dLeu2* gene does not affect the correct splicing of the dLeu2 transcript.

(E) Deletion of the *lox*P-flanked *MDR* allele in vivo. Southern blot analysis of SpeI-digested DNA from purified $CD19^+$ B cells of $MDR^{fl/+}$CD19-Cre and $MDR^{fl/+}$ mice. $MDR^{fl/+}$ CD19-Cre mice show the WT allele and the allele after *lox*P-mediated deletion.

(F) Deletion of the *lox*P-flanked *miR-15a/16-1* allele in vivo. PCR analysis from purified $CD19^+$ and $CD19^-$ B cells. CD19-enriched B cells from *miR-15a/16-1*$^{fl/+}$ CD19-Cre mice have the WT allele and the allele obtained after *lox*P-mediated deletion, whereas those from *miR-15a/16-1*$^{fl/+}$ mice show the *lox*P-flanked and the WT allele; the faint *lox*P-deleted band in the CD19-negative *miR-15a/16-1*$^{fl/+}$CD19-Cre fraction is due to cellular contamination of B cells.

referred to as *miR-15a/16-1*$^{+/-}$ mice. Reverse transcriptase-polymerase chain reaction (RT-PCR) analysis of purified $CD19^+$ splenic B cells for *dLeu2* confirmed that normal dLeu2 mRNA expression was not perturbed in mice with a homozygous deletion of *miR-15a/16-1* (Figure 1D). The conditional *miR-15a/16-1* allele was confirmed to express physiological amounts of the miRs (Figure S1B3). To generate age-matched cohorts of *MDR*- or *miR-15a/16-1*-homozygous, heterozygous, and wild-type littermates, we intercrossed the F1 generation of $MDR^{+/-}$ or *miR-15a/16-1*$^{+/-}$ mice. Both genotypes yielded homozygous mice at the expected Mendelian frequencies.

$CD5^+$ B Cell Expansion in $MDR^{-/-}$ and *miR-15a/16-1*$^{-/-}$ Mice

Mice of both recombinant genotypes developed normally and macroscopic and microscopic analysis showed that nonlymphoid organs including heart, lung, liver, kidney, and intestine of $MDR^{-/-}$ or *miR-15a/16-1*$^{-/-}$ mice were normal. At young

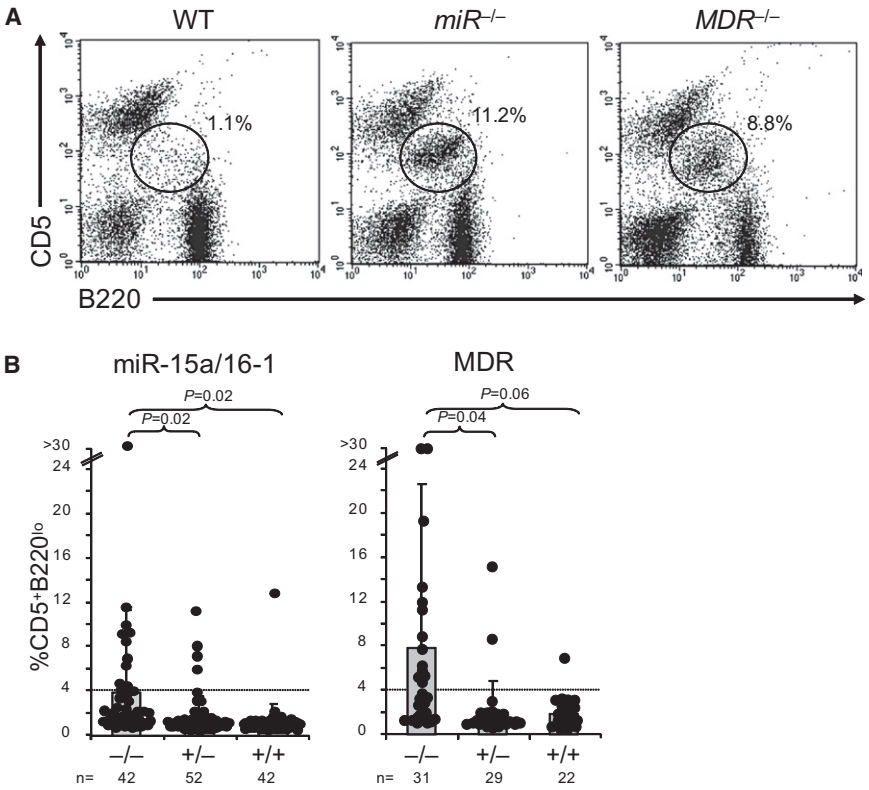

Figure 2. CD5⁺ B Cell Expansions in PB of Mice with Deletion of *MDR* or *miR-15a/16-1*

(A) Flow cytometry of PB mononuclear cells from a *miR-15a/16-1*$^{-/-}$, an *MDR*$^{-/-}$, and an age-matched WT mouse for CD5 and the B cell marker B220. The two former mice display a distinct CD5^{+}B220^{lo} population that does not occur in WT mice.

(B) Percentages of CD5^{+}B220^{lo} cells among mononuclear cells of mice from MDR and miR-15a/16-1 cohorts; "n" refers to the number of mice analyzed, p values (t test) are indicated; the dotted line demarks the upper threshold for the normal range of CD5^{+}B220^{lo} cells in a panel of 3- to 6-month-old WT mice determined by the average percentage ± 3σ; percentages above 4% are considered CD5^{+} lymphocytosis. Data are shown both as actual values (filled circles) and as mean and standard deviation (± SD).

age (2–4 months), homozygous *MDR*$^{-/-}$ and *miR-15a/16-1*$^{-/-}$ mice showed normal percentages of B cell and T cell subpopulations and normal development of lymphoid organs (Figure S2A and data not shown). Immunization of 2- to 3-month-old *MDR*$^{-/-}$ mice with a T cell-dependent antigen showed no differences in the percentages of the responding cell types, including germinal center (GC) B cells, IgG1^{+} memory B cells, and plasma cells (Figure S2B). Together, these results suggest that homozygous deletion of the *MDR* or *miR-15a/16-1* does not impair lymphocyte development in young mice. However, at 12 months of age, *MDR*$^{-/-}$ mice showed higher percentages of CD5^{+}B220^{low} B cells among mononuclear cells (MNC) in the peritoneal cavity (PerC) (~50% versus ~15% in controls; Figure S2C, top), which were poly/oligoclonal by flow cytometric analysis (data not shown). A trend toward higher fractions of PerC CD5^{+}B220^{low} B cells in *MDR*$^{-/-}$ mice was already detectable at 9 months. Similar observations were made in *miR-15a/16-1*$^{-/-}$ mice (Figure S2C, bottom). Thus, deletions of the *MDR* and miR-15a/16-1 are associated with expansion of CD5^{+}B220^{low} cells in the PerC, suggesting that the *MDR* locus has a role in regulating the pool of mature CD5^{+} B cells.

Deletion of *MDR* or *miR-15a/16-1* Leads to MBL

With increasing age (15–18 months), flow cytometric analysis of various MNC populations in the peripheral blood (PB) revealed that *MDR*$^{-/-}$ and *miR-15a/16-1*$^{-/-}$ mice frequently developed a CD5^{+}B220^{low} population in the PB (Figure 2A), which was shown to be clonal by PCR amplification and direct sequencing of rearranged IgV genes (Table S1). This population accounted for ~8% and ~4% of PBMC in *MDR*$^{-/-}$ and *miR-15a/16-1*$^{-/-}$ mice, respectively (Figure 2B). At lower penetrance, the same phenotype was detectable also in both *MDR* and *miR-15a/16-1* monoallelic-deleted mice, although the difference compared with wild-type mice did not reach statistical significance. These results demonstrate that deletion of the *MDR* or *miR-15a/16-1* promotes the development of clonal lymphocytosis in the PB, which in a percentage of cases was restricted to the PB analogous to human MBL. Approximately 5% of both *MDR*$^{-/-}$ and *miR-15a/16-1*$^{-/-}$ mice developed MBL (see Figure 4A).

Development of CLL and Non-Hodgkin Lymphoma in *MDR* and *miR-15a/16-1*-Deleted Mice

In a fraction of mice, clonal CD5^{+} B cell populations were accompanied by significant infiltration of lymphoid organs, as detected by flow cytometry and/or Southern blot analysis for IgH rearrangements, with histopathologic features resembling human CLL/small cell lymphocytic leukemia (SLL) (Figure 3). These mice displayed an enlargement of the splenic white pulp due to the expansion or accumulation of small lymphocytes, with a pattern similar to CLL/SLL (Figure 3 and Figure S3A). The PB smear displayed abundant small lymphocytes and numerous "smudge cells" characteristic of human CLL (Figure 3 bottom) Discrete aggregates of small lymphocytes could also be observed in the bone marrow (Figure S3A). Southern blot analysis demonstrated that these lymphoproliferations were clonal (Figure S3B). Overall, 27% of *MDR*$^{-/-}$ and 21% of *miR-15a/16-1*$^{-/-}$ mice developed CLL/SLL (see Figure 4A).

Finally, a fraction of mice of both genotypes developed clonal CD5-negative NHL of splenic and/or lymph node origin (9% of *MDR*$^{-/-}$, 17% of *MDR*$^{+/-}$, and 2% of *miR-15a/16-1*$^{-/-}$ mice) (Figure 3, right, Figure 4). Some of these tumors showed a mature B cell phenotype (IgM^{+} or Ig isotype switched, with a few staining for GC B cell markers [peanut agglutinin, PNA]) histologically reminiscent of human DLBCL, whereas a minority of tumors showed plasmacytic features similar to lymphoplasmacytic lymphoma in humans (data not shown).

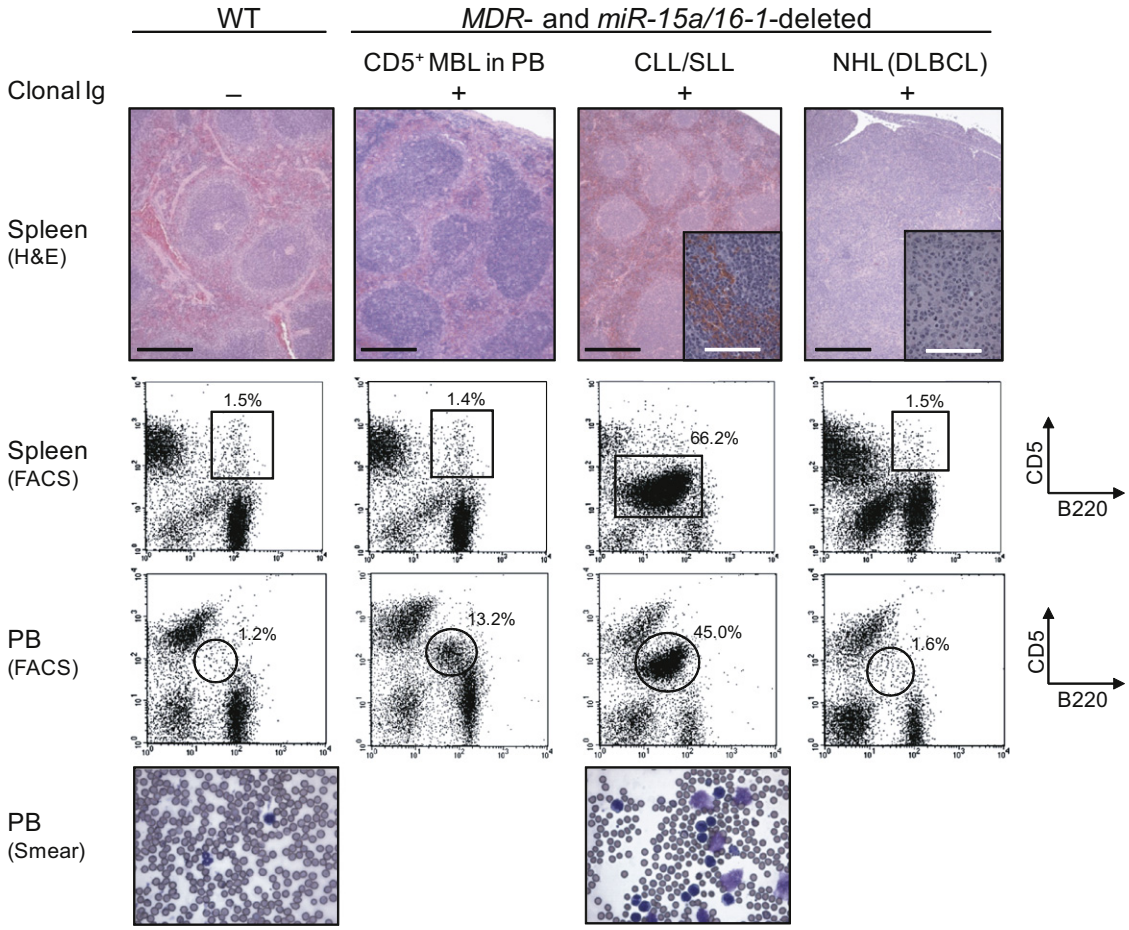

Figure 3. Clonal Lymphoproliferations in Mice with Deletion of *MDR* or *miR-15a/16-1*

The top row shows representative hematoxylin and eosin (H&E) stained spleen sections from *MDR*- or *miR-15a/16-1*-deleted mice presenting with MBL (from a 15-month-old *miR-15a/16-1*$^{-/-}$ mouse), CLL/SLL (from a 17-month-old *MDR*$^{-/-}$ mouse), or DLBCL (from a 17-month-old *MDR*$^{+/-}$ mouse), and an age-matched WT mouse (left). CLL/SLL: section shows enlargement of the splenic white pulp by the expansion or accumulation of small B lymphocytes with architectural and morphologic features of CLL/SLL. DLBCL: section shows lymphoid tissue with an infiltrate of large lymphocytes with morphologic features of DLBCL. The scale bar represents 1000 μm; the scale bar in the inset represents 100 μm. The second and third row show flow cytometry of splenic and PBMC cells from the corresponding mice for CD5 and the B cell marker B220. The CLL/SLL case shows a predominant CD5^{+}B220^{lo} population in spleen and PB, the MBL case demonstrates this population only in the PB. The bottom row shows Wright-Giemsa stained PB smear showing an abundance of small lymphocytes and "smudge cells" from a mouse diagnosed with CLL/SLL, compared with an age-matched WT mouse (left).

MDR$^{-/-}$ Mice Have a More Aggressive Disease Course than *miR-15a/16-1*$^{-/-}$ Mice

Altogether 42% of *MDR*$^{-/-}$ and 26% of *miR-15a/16-1*$^{-/-}$ 15- to 18-month-old mice developed clonal B cell lymphoproliferations, including CD5^{+} MBL, CLL/SLL, and NHL (Figure 4A). *MDR*$^{+/-}$ mice too showed a trend toward developing B cell tumors (24%), suggesting that monoallelic deletion of the MDR can cause disease. This trend is not evident in *miR-15a/16-1*-deleted mice, probably due to the lower penetrance of the phenotype.

The event-free survival curves showed that *MDR*$^{-/-}$ mice died earlier than their wild-type littermates ($p = 0.002$), suggesting that the homozygous mice eventually succumb to their tumors at an advanced age. Conversely, the event-free survival of *miR-15a/16-1*$^{-/-}$ mice was not different from wild-type littermates, suggesting that these mice show a significantly milder disease course than their MDR counterparts (Figure 4B). In conclusion, both *MDR*$^{-/-}$ and *miR-15a/16-1*$^{-/-}$ mice developed lymphoproliferations with an indolent disease course reminiscent of human CLL, with the *MDR*$^{-/-}$ mice displaying a more aggressive disease phenotype.

Lymphoproliferations in *MDR* and *miR-15a/16-1*-Deleted Mice Are B Cell Autonomous

MDR$^{-/-}$ and *miR-15a/16-1*$^{-/-}$ mice carry the respective deletions in all cells, leaving open the possibility that the observed lymphoproliferations may be due to the effect of the deletions in non-B cells. To investigate whether the proliferations observed in those mice developed in a B cell-autonomous fashion, we generated mice that specifically delete either the *MDR* or the *miR-15a/16-1* allele in B cells by crossing *MDR*$^{loxP\text{-}frt/+}$ or *miR-15a/16-1*$^{fl/+}$ mice with mice in which the Cre recombinase is under transcriptional control of the B-lineage-restricted gene encoding CD19 (CD19-Cre mice); these mice are further on

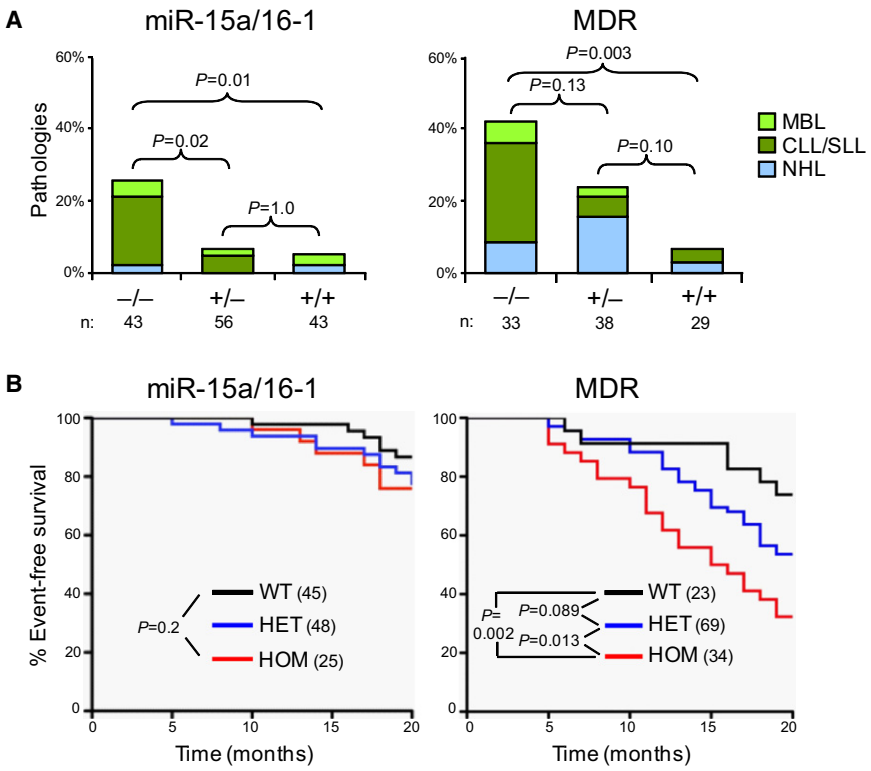

Figure 4. Mice with Germline Deletion of *MDR* or *miR-15a/16-1* Develop Lympho-Proliferations at Low Penetrance and Show an Indolent Disease Course

(A) Percentages of B-lymphoid pathologies observed in 15- to 18-month-old mice of the MDR or miR-15a/16-1 cohorts. The percentages of MBL, CLL/SLL, and NHL in each genotype are color coded. "n" refers to the number of mice analyzed; p values (chi-square test of association) among the genotypes are indicated. Data are shown both as actual values (filled circles) and as mean ± SD. The lymphoproliferations occurred in two independent *miR-15a/16-1*$^{-/-}$ mouse lines (data not shown).

(B) Percent event-free survival in the MDR or miR-15a/16-1 cohorts. Mice were followed for duration of 20 months. Events comprised mice that succumbed to illness or those identified as moribund or sick (palpable tumor or visible ascitis) and thus sacrificed. The p values between the different genotypes of the *MDR* cohort, and those between *miR-15a/16-1* homozygous and WT mice, are indicated. The number of mice of each genotype is indicated in brackets. Mice shown in Figures 4A and 4B corresponded to different cohorts.

referred to as *MDR*$^{fl/+}$CD19-Cre or *miR-15a/16-1*$^{fl/+}$CD19-Cre mice. Southern blot or RT-PCR analysis of purified CD19$^+$ B cells demonstrated the ability of the conditional *MDR* and *miR-15a/16-1* alleles to recombine in vivo (Figures 1E and 1F).

We generated cohorts of *MDR*$^{fl/-}$CD19-Cre or *miR-15a/16-1*$^{fl/-}$CD19-Cre mice that delete both alleles only in B cells, and the corresponding heterozygous and wild-type controls, i.e., *MDR*$^{+/-}$CD19-Cre and CD19-Cre, or *miR-15a/16-1*$^{+/-}$CD19-Cre and CD19-Cre littermates. The results demonstrated that 15-18-month-old *MDR*$^{fl/-}$CD19-Cre and *miR-15a/16-1*$^{fl/-}$CD19-Cre mice presented with CD5$^+$ B cell lymphocytosis in the PB (Figure 5A), and showed the same spectrum of B cell pathologies, at comparable frequencies, as observed in the corresponding constitutional knock-out mice (Figure 5B). Taken together, the results suggest that the development of clonal lymphoproliferations in *MDR*- or *miR-15a/16-1*-deleted mice occurred in a B cell-autonomous fashion.

Stereotypical Antigen Receptors in CD5$^+$ Lymphoproliferations

Sequence analysis of PCR-amplified IgV genes from tumors of homo- or heterozygous *MDR* or *miR-15a/16-1* mice demonstrated that CD5$^+$ tumors expressed unmutated IgV genes, whereas the CD5$^-$ NHLs mostly expressed somatically mutated IgV genes (Table S1). These results suggest that lymphoproliferations in the *MDR*- or *miR-15a/16-1*-deleted mice originated from B cells participating in T cell-independent and -dependent antibody responses.

A distinctive feature of human CLL is the expression of structurally identical or similar BCR heavy-chain complementary determining regions 3 (HCDR3) resulting from the recombination of the V_H, D_H, and J_H gene segments between unrelated individuals (HCDR3 "stereotypy" [Messmer et al., 2004; Tobin et al., 2004; Widhopf et al., 2004]; for review see Ghia et al., 2008). We compared the amino acid sequences of the HCDR3 regions among the B cell tumors and observed that although the CD5$^-$ NHL cases showed highly variable HCDR3 regions (Table S2), we could identify several clonal CD5$^+$ B cell proliferations that expressed IgV genes using the same V_H and J_H families and in addition showed highly similar HCDR3 regions ($\geq$80% homology at the protein level (Yan et al., 2006)) (Table 1). These results suggest that CD5$^+$ B cell lymphoproliferations in *MDR* and *miR-15a/16-1*-deleted mice can express antibodies with stereotypical antigen binding regions, suggesting a role for common antigens or autoantigens in the clonal expansion, analogous to human CLL (Ghia et al., 2008).

miR-15a/16-1 Control Proliferation in Mouse and Human B Cells

To understand the mechanism by which the deletions lead to clonal B-lymphoproliferations, we investigated whether miR15-a/16-1-deletions could affect proliferation of mouse B cells, as previously suggested for nonlymphoid cells (Bandi et al., 2009; Calin et al., 2008; Linsley et al., 2007; Liu et al., 2008; Raveche et al., 2007). BrdU incorporation assays, which measure active DNA-synthesis, demonstrated that *miR-15a/16-1*$^{-/-}$ B cells begin to synthesize DNA earlier than wild-type B cells (Figure 6A). Mitogen-stimulated B cells purified from *miR-15a/16-1*$^{-/-}$ or *MDR*$^{-/-}$ and wild-type mice were analyzed for the levels of phosphorylated retinoblastoma (p-Rb) protein, which represents an indicator of cell cycle entry, because p-Rb cannot repress the growth-promoting gene E2F (Weintraub et al., 1992).

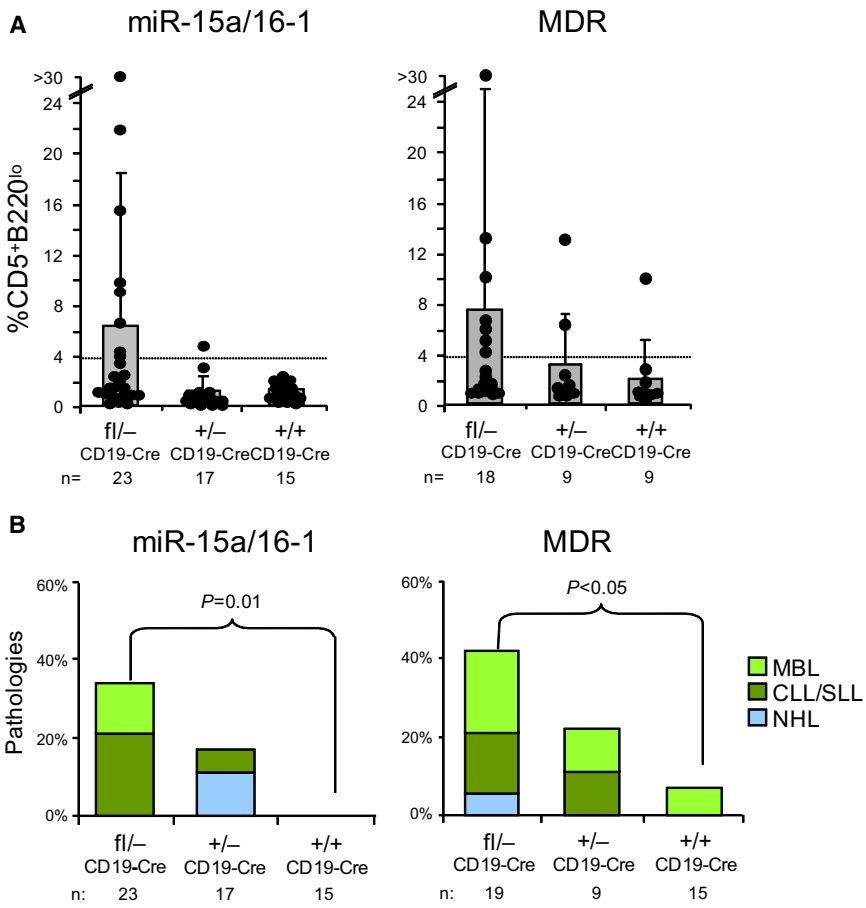

Figure 5. Mice with Deletion of *MDR* or *miR-15a/16-1* Develop Lymphoproliferations in a B Cell-Autonomous Fashion

(A) Percentages of $CD5^+B220^{lo}$ cells among mononuclear cells of 15- to 18-month-old mice from MDR- and miR-15a/16-1-CD19-Cre cohorts; n, number of mice analyzed; for definition of the dotted line, see legend to Figure 2. For some cases shown in (B), PB was not analyzed. Data are shown both as actual values (filled circles) and as mean ± SD.

(B) Percentages of B-lymphoid pathologies observed in 15- to 18-month-old mice of the MDR- or miR-15a/16-1-CD19-Cre cohorts. Mice were sacrificed and analyzed for pathologies. The percentages of MBL, CLL/SLL, and NHL in each genotype are color-coded. n, number of mice analyzed; p values (chi-square test of association) among the genotypes were indicated if ≤ 0.05.

The results showed that p-Rb could be detected at earlier time points in both *miR-15a/16-1*$^{-/-}$ and *MDR*$^{-/-}$ compared with wild-type B cells (Figure 6B, and Figure S4A). Consistent with this observation, expression of the cell-cycle inhibitory protein cyclin-dependent kinase inhibitor p27-Kip1 appeared to follow similar kinetics (Figure 6B). Moreover, results from experiments that determined the number of cell divisions following mitogen-stimulation (CFSE incorporation; Figure S4B) showed that *MDR*-deleted cells begin to proliferate earlier than wild-type B cells. Of note, we did not observe differences in the proliferative response between animals in a *129/Sv-C57BL/6* mixed and a *C57BL/6* pure background (data not shown), suggesting that the observed phenotype is not associated with a specific genetic background.

To further unravel the individual contributions of *DLEU2* versus the *miR-15a/16-1* cluster to the lymphoproliferative phenotype, we generated an inducible in vitro system in which the DLEU2 transcript and the miR-15a/16-1 cluster were separately re-expressed in the human I83E95 cell line that is derived from a 13q14$^{-/-}$ CLL (Wendel-Hansen et al., 1994). We used an expression vector in which a doxycycline-inducible promoter drives the bidirectional transcription of GFP and the inserted sequences (Figures 6C–6F). The results showed that miR-15a/16-1-expressing cells, but not those expressing DLEU2, were impaired in proliferation (Figure 6G). Consistent with this observation, miR-15a/16-1-expressing cells had a higher fraction of cells in the G_0/G_1 phase compared with both DLEU2 and the control as documented by BrdU incorporation assays (Figure 6H). Thus, expression of the miR-15a/16-1 cluster seems to control cellular proliferation, possibly by inhibiting the G_0/G_1–S phase transition. Taken together, the results of the knock-out and re-expression experiments suggest that the miR-15a/16-1 cluster exhibits negative control of proliferation

Table 1. $CD5^+$ Lymphoproliferations from *MDR*, *miR-15a/16-1*-Deleted, or Wild-Type Mice Show Similar HCDR3 Sequences

Animal	V_H	V_H	N	D_H	N	J_H	J_H	CDR3 Length	Diagnosis
miR	CD19-Cre #10	V328	A		IYYGN	YWYFDV	1	12	CLL/SLL
MDR	CD19Cre #99	V328	AR		YYSN	YWYFDV	1	12	CLL/SLL
miR^f	CD19Cre #234	V328	AR	GEK	YSN	YWYFDV	1	14	CLL/SLL
MDR	#27	V235	MR		YSN	YWYFDV	1	11	CLL/SLL
MDR$^-$	#138	V153	MR		YGN	YWYFDV	1	11	CLL/SLL
MDR	CD19-Cre #197	V227	A	SP	NWD	YWYFDV	1	11	MBL
MDR	CD19-Cre #212	V186	AR		NWD	YWYFDV	1	10	MBL

Data for *MDR*, *miR-15a/16-1*-deleted, or wild-type mice are grouped in the following cases, respectively: #10, #99, and #234; #27 and #138; and #197 and #212. Cases that showed ≥80% amino acid sequence homology in the HCDR3 are grouped (cases #10 and #99, and cases #99 and #234 show ≥80% homology).

both in human and mouse B cells. On the contrary, the DLEU2 transcript per se did not affect proliferation of 13q14-homozygous deleted cells.

Identification of Potential miR-15a/16-1 Target Genes in B Cells

Our results suggested that miR-15a/16-1 may affect the G_0/G_1-S phase transition in B cells (see Figure 6). We thus sought to identify candidate G_0/G_1-S phase-related genes among inferred miR-15a/16-1 targets. Among those predicted by at least one of four established computational target prediction algorithms (miRanda, PicTar, TargetScan, and RNA22; see Experimental Procedures), nine proteins were known to be critically involved in the regulation of the G_0/G_1-S phase transition, including cyclins CCND1, CCND2, CCND3, and CCNE1, and cyclin-dependent kinases CDK4, CDK6, CHK1, MCM5, and CDC25A. Three of these (CCND3, CCNE1, and CDK6) constitute verified miR-15a/16-1 targets in nonlymphoid systems (Liu et al., 2008) (CCND1 is not expressed in B cells and therefore not considered here); the computational target prediction algorithms by which the remaining miR-15a/16-1 targets were identified and the number of potential binding sites per gene are summarized in Table S3 (see also Figure S5; the 3′UTRs of the corresponding genes are listed in Table S4). With the exception of CDC25A, all proteins were downregulated in I83E95 13q14$^{-/-}$ cells upon miR-15a/16-1 expression (Figure 7A middle, and Figure S6A). Analogously, all gene products except Cdc25A showed higher expression levels in anti-IgM-stimulated miR-15a/16-1-deficient mouse B cells; of note, Ccnd2, Ccnd3, Cdk4, Cdk6, and Chk1 were upregulated faster and at markedly increased levels in *miR-15a/16-1*$^{-/-}$ versus wild-type B cells (Figure 7A middle). Although it remains to be determined whether the proliferation-associated genes identified represent direct or indirect miR-15a/16-1 targets, the concurrent results obtained in two independent genetically defined miR-15a/16-1 knock-out systems strongly indicate that those microRNAs regulate their expression. In conclusion, the *miR-15a/16-1* cluster seems to negatively regulate the expression of multiple genes involved in the G_0/G_1-S phase transition in both human and mouse B cells.

We also performed a supervised gene expression profile (GEP) analysis of I83E95 cells stably transfected with miR-15a/16-1 or empty-vector and validated the candidates at the protein level (for details, see Supplemental Information). The results showed additional proteins as clearly affected by miR-15a/16-1 induction (Figure 7A, middle, and Figure S6B; Table S3 and Figure S5), including CCNE1 and CSE1L which are associated with cell growth/proliferation (Behrens et al., 2003), IGF1R, an antiapoptotic receptor (Fürstenberger and Senn, 2002), and ARL2, involved in cytokinesis (Burd et al., 2004). Interestingly, c-MYB, which has been reported as a miR-15a/16-1 target in nonlymphoid cells (Zhao et al., 2009) was confirmed in this assay. Conversely, we observed only a modest reduction of BCL2 protein (~2-fold), whose regulation by miR-15a/16-1 has been controversial (Cimmino et al., 2005; Fulci et al., 2007; Linsley et al., 2007) (Figure 7A bottom, and Figure S6A for quantification, see also Figure S7B). Immunohistochemical analysis of spleen sections for BCL2 expression showed the characteristic staining pattern with GC B cells being BCL2-negative in both wild-type and *miR-15a/16-1*$^{-/-}$ mice (Figure S7A), suggesting that a miR-15a/16-1-mediated control of BCL2-expression may have only limited functional relevance in normal B cell physiology.

Taken together, the present findings suggest that a major role of the tumor suppressor in chromosomal region 13q14 is the control of cell proliferation. Specifically, deletion of the *miR-15a/16-1* cluster in B cells may accelerate the G_0/G_1-S phase transition by failing to negatively regulate the expression of molecules critically involved in this transition (Figure 7B).

DISCUSSION

These results show that the *DLEU2/miR-15a/16-1* locus plays an important role in controlling the expansion of the mature B cell pool. The mechanism by which this control is exerted is mainly by downregulation of genes controlling cell cycle entry. The in vivo evidence presented here corroborates and expands on previous observations obtained in vitro mostly in non-B cells (Bandi et al., 2009; Calin et al., 2008; Cimmino et al., 2005; Linsley et al., 2007; Liu et al., 2008; Raveche et al., 2007), and suggests that the *DLEU2/miR-15a/16-1* locus controls B cell expansion primarily by modulating proliferation, rather than by influencing survival via regulation of BCL2. Importantly, despite its expression in many tissues, the function of the *DLEU2/miR-15a/16-1* locus appears to be critical mainly for B cells because no clearly abnormal phenotype was detectable in other cell types. This apparent specificity may be explained by the need to tightly modulate the entry of B cells into the cell cycle in response to a broad range of *low affinity* stimulation by extrinsic antigens and/or autoantigens. This hypothesis is supported by the observation that DLEU2/miR-15a/16-1 expression is downregulated in proliferating B cells within the germinal centers in vivo, the site where B cells are selected for the production of antibodies with *high affinity* for the antigen (unpublished observation).

These results also establish that the *DLEU2/miR-15a/16-1* locus has a tumor-suppressor role in the B cell lineage in vivo, providing a paradigm for a similar role for other sterile transcripts in human diseases. Within this locus, one active genetic element is clearly the *miR-15a/16-1* cluster, based on its antiproliferative effect in vitro, its targeting of cell cycle genes, and the lymphoproliferative phenotype of *miR-15a/16-1*-deleted mice. However, the significantly more aggressive phenotype displayed by the *MDR*-deleted mice (both in constitutionally deleted and conditionally deleted mice) suggests that additional genetic elements within the *MDR* locus contribute to the tumor suppressive function. One candidate for such a role is *DLEU2* itself. Besides providing the primary transcript for the production of miR15a/16-1, it produces a spliced cytoplasmic RNA (data not shown) that, analogous to other long sterile transcripts (Ponting et al., 2009), may have important regulatory functions not detected by the in vitro assays used here. Alternatively, the *DLEU5* gene, although excluded from the *MDR* in humans, may have a tumor-suppressor role in the mouse, which, due to partially overlapping loci in the mouse genome (see Figure 1A), could not be distinguished from the one of *DLEU2/miR-15a/16-1*. It is, however, important to note that 13q14 deletions are commonly large and invariably involve the entire *DLEU2/miR-15a/16-1* locus, thus suggesting that the genetic element within the *MDR* that contributes to the phenotype of the *miR-15a/16-1*-deleted

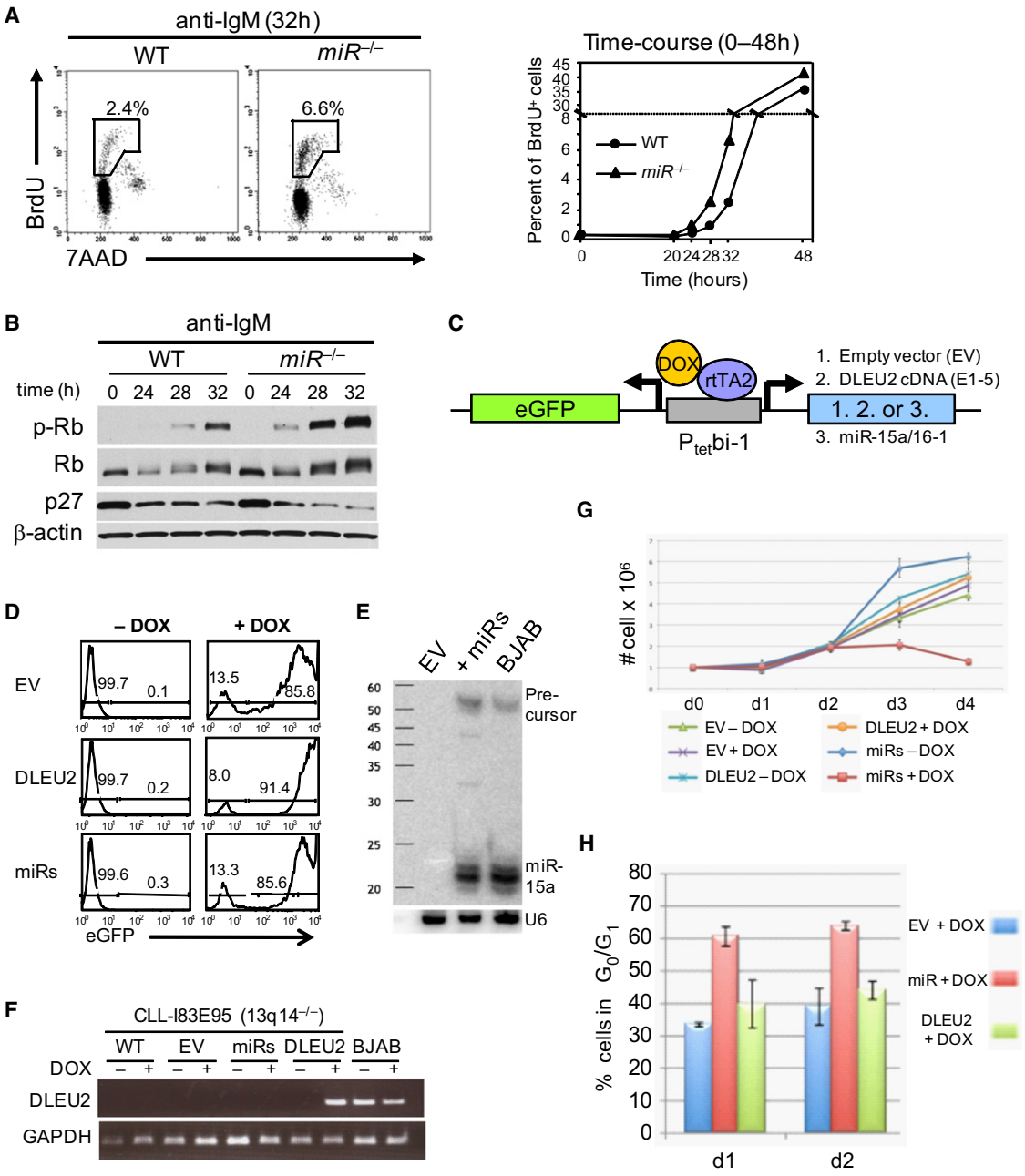

Figure 6. miR-15a/16-1 Expression Impairs Proliferation in B Cells

(A) *miR-15a/16-1*$^{-/-}$ B cells show earlier cell cycle entry than WT B cells. (Left) Representative flow cytometry of a BrdU-incorporation experiment at time point 32 hr. Cultures of anti-IgM-stimulated cells were incubated for 30 min before harvesting for BrdU/7AAD analysis. (Right) Representative time course of a BrdU-incorporation experiment with *miR-15a/16-1*$^{-/-}$ (*miR*$^{-/-}$) and WT B cells. We observed variations in the actual timing of proliferation initiation between individual experiments.

(B) *miR-15a/16-1*$^{-/-}$ B cells show faster phosphorylation of Rb protein than WT B cells. Purified B cells of the corresponding genotypes were stimulated by anti-IgM Fab-fragments and harvested at the indicated time points. Western blots probed with an anti-p-Rb and with an anti-Rb antibody are shown; the higher bands in the Rb-blot correspond to phosphorylated Rb.

(C) Scheme of a vector that expresses miR-15a/16-1 or DLEU2 (exons 1–5) along with GFP from a doxycycline-inducible bidirectional promoter; transcriptional orientation of the respective genes is indicated.

(D) Addition of doxycycline to stable cell lines containing either of the indicated genes or empty vector (EV) results in eGFP expression in the majority of cells, and at equal percentages among the different stably transfected I83E95 cell lines, demonstrating the efficiency of the inducible system.

(E) miR-15a was selectively expressed in doxycycline-induced miR-15a/16-1-stably transfected I83E95 cells, as demonstrated by Northern blot analysis. BJAB was included as positive control. U6 RNA was probed to test for RNA quality and equal loading of the samples.

(F) DLEU2 mRNA was selectively expressed in doxycycline-induced DLEU2-stably transfected I83E95 cells, as demonstrated by RT-PCR.

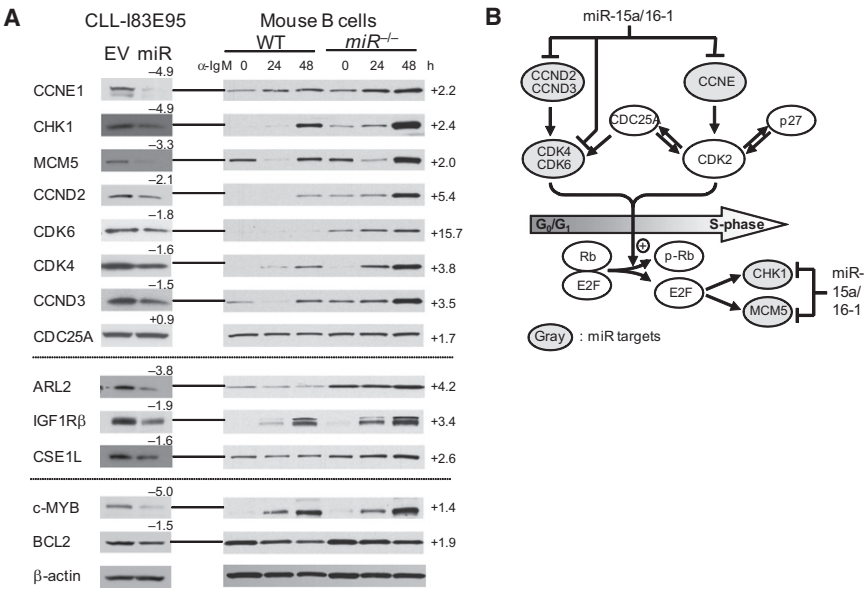

Figure 7. Identification of miR-15a/16-1 Targets in B Cells

(A) Functional analysis for miR-15a/16-1-dependent protein expression changes of putative targets identified by (1) computationally predicted miR-15a/16-1-targets implicated in the G_0/G_1-S transition (top), (2) gene expression profiling (GEP) (middle), and (3) the known targets c-MYB and BCL2 (bottom), by either reintroduction of miR-15a/16-1 into the 13q14$^{-/-}$ human cell line CLL-I83E95 (left), or deletion of *miR-15a/16-1* in mouse B cells (right). Fold changes in protein expression observed upon reintroduction of miR-15a/16-1 are indicated (left); average from two independent experiments. The expression of miR-15a/16-1-targets was analyzed in a time-dependent fashion in resting (0 hr) and IgM-stimulated proliferating mouse B cells (24 hr and 48 hr) purified from spleens of *miR-15a/16-1*$^{-/-}$ mice and WT littermates (right) (representative experiment; for quantification, see Figure S5). Fold changes in protein expression at time points 24 hr (top) or 48 hr (middle, bottom) are indicated. The figure shows a representative β-actin blot; for quantification, the β-actin blots of the corresponding filters were used. Bars between Western blots indicate concordant miR-15a/16-1-dependent expression changes in human and mouse B cells. (B) Model incorporating the results shown in Figures 6 and 7A: miR-15a/16-1 downregulate the expression of several proliferation associated proteins that have important roles in the G_0/G_1-S phase transition. The absence of miR-15a/16-1 causes a faster or stronger activation of CCND2 and CCND3 as well as CDK4 and CDK6, which are critical cell cycle checkpoints, as well as CCNE, thus leading to faster phosphorylation of Rb and hence accelerated entry into cell cycle by activating E2F. Likewise, the E2F-regulated cell cycle-associated proteins CHK1 and MCM5 may contribute to the pro-proliferative phenotype of miR-15a/16-1-deficient cells. miR-15a/16-1 targets are indicated by light blue ovals.

mice is ablated in the *MDR*-deleted mice. The notion that *DLEU5* may play a role in determining the lymphoproliferative phenotypes opens the possibility that 13q14 deletions of different size, i.e., including or excluding the *DLEU5* locus, may influence the aggressiveness of the CLL phenotype in humans.

Several features of the lymphoproliferative phenotype observed in the *MDR*-deleted mice indicate that these mice represent a remarkably faithful model of human CLL. First, this model has been generated by recapitulating the genetic lesion associated with the human disease. Previous mouse models of CLL were represented by transgenic mice expressing a dominantly acting oncogene (TCL1) (Bichi et al., 2002) not clearly associated with a genetic lesion in human B cell neoplasms, or by a mouse strain (NZB) in which the phenotype was linked to multiple loci (Raveche et al., 2007) and the role of miR-15a/16-1 could not be conclusively demonstrated. Second, these mice display the full spectrum of CLL-associated phenotypes, including MBL, the presumed low-penetrance premalignant stage, classic CLL/SLL, and the low-penetrance aggressive progression stage DLBCL. Third, the observed clonal CD5$^+$ phenotypes display "stereotypic" Ig gene usage, a very specific feature of human CLL that suggests an important role for extrinsic antigens or autoantigens. Finally, the lymphoproliferative diseases displayed by the *MDR*-deleted mice are indolent and have low penetrance, as expected for a model of human CLL, a malignancy with a typically indolent course that is significantly more common in the elderly population. It is noteworthy, however, that the penetrance of the phenotypes may be underestimated in this study because the mice have been kept in virtually germ-free conditions, whereas antigen exposure from various infectious agents has been repeatedly suggested as a cofactor in CLL development. Overall, these observations indicate that the mouse model described here may be useful for the study of disease progression in CLL and as a preclinical model for testing new therapeutic regimens for this disease.

EXPERIMENTAL PROCEDURES

Generation of *MDR* and *miR-15a/16-1* Conditional and Null Mice

For a detailed description of the transgenic mouse generation, see Figure S1 and Supplemental Experimental Procedures. In brief, two targeting vectors were devised in order to flank the *MDR* with *lox*P and *frt*-sites. Successively inserted into the cloning sites of the corresponding 5′ tag and 3′ tag vectors were each two DNA fragments of the *129/Sv-14qC3*. To generate a conditional *miR-15a/16-1* allele, successively inserted into the cloning sites of the targeting vector were three DNA fragments of the *miR-15a/16-1*-locus. Chimeras were obtained from correctly targeted ES cell colonies after injection of the targeted W9.5 ES clones (*129/SvEvTac*) into blastocysts derived from *C57BL/6* mice, and gave rise to *MDR*$^{fl/+}$ or *miR-15a/16-1*$^{fl/+}$ mice. The chimeras were

(G) Reintroduction of miR-15a/16-1 into I83E95 cells impairs proliferation. Stably transfected cell lines that allow the expression of miR-15a/16-1, DLEU2, or empty vector (EV) in a doxycyclin-dependent fashion were cultured with or without doxycycline and cell numbers were determined at the indicated time points. (H) Reintroduction of miR-15a/16-1 into I83E95 cells causes accumulation of cells in G_0/G_1. Cell cycle profile and percentage of cells actively synthesizing DNA upon expression of miR-15a/16-1, DLEU2, or EV were determined by BrdU incorporation/7AAD assay. The experiment shown in (G) and (H) were each performed twice; data are shown as mean ± SD.

also crossed with *129/Sv*$^{CAGGS\text{-}Flpe}$ or *129/Sv*$^{Zip3\text{-}Cre}$ mice (both Jackson Laboratories) to generate an *MDR* and a *miR-15a/16-1* null allele, respectively. Thus obtained *MDR*$^{+/-}$ or *miR-15a/16-1*$^{+/-}$ mice were crossed to *C57BL/6* mice, and the resulting F1 generation was intercrossed for establishing the experimental cohort. Likewise, *MDR*$^{fl/+}$ or *miR-15a/16-1*$^{fl/+}$ mice were bred with *C57BL/6* mice; those mice were intercrossed with CD19-Cre. In vivo deletion of the *lox*P-flanked *MDR* allele was verified by Southern blot analysis of purified B cells derived from *MDR*$^{fl/+}$CD19-Cre mice (Figure 1E). To test whether dLeu2 mRNA expression is affected upon deletion of *miR-15a/16-1*, purified B cells from *miR-15a/16-1*$^{-/-}$ and wild-type mice were tested for dLeu2 expression by RT-PCR, and in vivo deletion of the *lox*P-flanked *miR-15a/16-1* allele was verified by multiplex PCR analysis of purified B cells derived from *miR-15a/16-1*$^{fl/+}$CD19-Cre mice (Figure 1F) (for primer sequences, see Supplemental Information). All experiments with mice were approved by the Institutional Animal Care and Use Committee (IACUC) of Columbia University, and all experiments conformed to the corresponding relevant regulatory standards.

Event-free Survival and Statistical Analysis

Tumor watch studies were conducted on animals in a *129/Sv-C57BL/6* mixed background (i.e., the first and second backcross generations). Mice were monitored for tumor incidence biweekly and were sacrificed when visibly ill. Within each transgenic line, comparable numbers of age-matched wild-type littermates controlled for possible differences in tumor incidence. Animals were monitored for up to 20 months. Statistical analysis was performed on the Prism 5 software program (GraphPad, San Diego, CA) using Kaplan-Meier cumulative survival and the log-rank (Mantel-Cox) test to determine whether differences were significant (Figure 4B). The χ^2 test was used to compare B-lymphoproliferation incidence between the different genotypes of the MDR and miR-15a/16-1 cohorts (Figures 4A and 5B).

IgM-Stimulation Assays

Purified B cells from *miR-15a/16-1*$^{-/-}$ or *MDR*$^{-/-}$ and wild-type mice were cultured at a density of 1.5 × 10^6 cells/ml in RPMI medium plus 10% FBS with 15 μg/ml goat-anti-mouse Fab fragments for up to 48 hr (Jackson Immunotech). For detection of pRb and miR-15a/16-1 predicted target proteins, cells were harvested at specific time points after stimulation, washed with phosphate-buffered saline, and stored as frozen pellets to enable simultaneous lysis of the samples for western blot analysis.

Doxycycline-Inducible miR-15a/16-1 and DLEU2 Expression in a 13q14$^{-/-}$ CLL Cell Line

DNA fragments encoding either miR-15a/16-1 or the exonic sequence of DLEU2 were inserted into the multiple cloning site of a doxycycline-inducible vector (Bornkamm et al., 2005). This vector allows constitutive expression of a bicistronic expression cassette encoding the doxycycline-sensitive reverse tetracycline controlled transactivator rtTA2^S-M2 and a Tet repressor-KRAB fusion protein (tTS^{KRAB})(silencer) located downstream of an internal ribosomal entry site. miR-15a/16-1 or DLEU2 are expressed from the bidirectional promoter P_{tet}bi-1, which allows simultaneous expression of those genes along with GFP that serves as surrogate marker for expression. The corresponding vectors were stably transfected into the 13q14$^{-/-}$ I83E95 cell line.

I83E95 cells were cultured in 20% FCS-IMDM media at 0.5 to 1 × 10^6 cells/ml density. Cells were electroporated (500 μF/220 V) and subsequently selected for the presence of the plasmids with hygromycin (250 μg/ml) for 12 days. Inducibility was assessed 24 hr after doxycycline addition by measuring GFP levels flow-cytometrically, DLEU2 transcript levels by RT-PCR and Northern blot, and miR-15a/16-1 levels by Q-RT-PCR and Northern blot.

miR-15a/16-1 Computational Target Prediction

Precompiled miRNA target predictions for human 3′UTR transcripts were downloaded from the respective website for each of the four algorithms: Pictar (http://pictar.mdc-berlin.de/), TargetScan (release 5.0, conserved sites, http://targetscan.org), Miranda (version 5, http://microrna.sanger.ac.uk/targets/v5), RNA22 (http://cbcsrv.watson.ibm.com/rna22.html). The union of the predictions by those algorithms was considered as the candidate miR-15a/16-1 target list.

BrdU-Incorporation Assay

For measurement of DNA synthesis in I83E95 cells or mouse B cells, cells were incubated with BrdU for 30 min at specific time points after the start of the culture, and immediately harvested and fixed. BrdU incorporation and DNA content were analyzed with the APC BrdU flow kit (Becton Dickinson). The cell suspensions were analyzed on a FACSCalibur using CellQuest software.

ACCESSION NUMBERS

Gene expression data have been deposited in the Gene Expression Omnibus (GEO) database with accession number GSE18866.

SUPPLEMENTAL INFORMATION

Supplemental Information includes Supplemental Experimental Procedures, seven figures, and four tables and can be found with this article online at doi:10.1016/j.ccr.2009.11.019.

ACKNOWLEDGMENTS

We thank H. Tang, P. Smith, and B. Chen for help with the pathology analysis; G. Cattoretti for initial characterization of the mouse models; T. Ludwig for advice in the construction of the transgenic mice; G. Bornkamm for providing the bicistronic expression cassette; and L. Pasqualucci, T. Rothstein, and A. Iavarone for discussion. We also thank the Flow Cytometry, Transgenic Mouse, and Genomics Shared Resources of the Herbert Irving Comprehensive Cancer Center.

Received: August 12, 2009
Revised: October 7, 2009
Accepted: November 9, 2009
Published online: January 7, 2010

REFERENCES

Avet-Loiseau, H., Li, J.Y., Morineau, N., Facon, T., Brigaudeau, C., Harousseau, J.L., Grosbois, B., and Bataille, R. (1999). Monosomy 13 is associated with the transition of monoclonal gammopathy of undetermined significance to multiple myeloma. Intergroupe Francophone du Myelome. Blood *94*, 2583–2589.

Bandi, N., Zbinden, S., Gugger, M., Arnold, M., Kocher, V., Hasan, L., Kappeler, A., Brunner, T., and Vassella, E. (2009). miR-15a and miR-16 are implicated in cell cycle regulation in a Rb-dependent manner and are frequently deleted or down-regulated in non-small cell lung cancer. Cancer Res. *69*, 5553–5559.

Baranova, A., Hammarsund, M., Ivanov, D., Skoblov, M., Sangfelt, O., Corcoran, M., Borodina, T., Makeeva, N., Pestova, A., Tyazhelova, T., et al. (2003). Distinct organization of the candidate tumor suppressor gene RFP2 in human and mouse: Multiple mRNA isoforms in both species- and human-specific antisense transcript RFP2OS. Gene *321*, 103–112.

Behrens, P., Brinkmann, U., and Wellmann, A. (2003). CSE1L/CAS: Its role in proliferation and apoptosis. Apoptosis *8*, 39–44.

Bichi, R., Shinton, S.A., Martin, E.S., Koval, A., Calin, G.A., Cesari, R., Russo, G., Hardy, R.R., and Croce, C.M. (2002). Human chronic lymphocytic leukemia modeled in mouse by targeted TCL1 expression. Proc. Natl. Acad. Sci. USA *99*, 6955–6960.

Bonci, D., Coppola, V., Musumeci, M., Addario, A., Giuffrida, R., Memeo, L., D'Urso, L., Pagliuca, A., Biffoni, M., Labbaye, C., et al. (2008). The miR-15a-miR-16-1 cluster controls prostate cancer by targeting multiple oncogenic activities. Nat. Med. *14*, 1271–1277.

Bornkamm, G.W., Berens, C., Kuklik-Roos, C., Bechet, J.M., Laux, G., Bachl, J., Korndoerfer, M., Schlee, M., Holzel, M., Malamoussi, A., et al. (2005). Stringent doxycycline-dependent control of gene activities using an episomal one-vector system. Nucleic Acids Res. *33*, e137.

Bullrich, F., Fujii, H., Calin, G., Mabuchi, H., Negrini, M., Pekarsky, Y., Rassenti, L., Alder, H., Reed, J.C., Keating, M.J., et al. (2001). Characterization of the

13q14 tumor suppressor locus in CLL: Identification of ALT1, an alternative splice variant of the LEU2 gene. Cancer Res. *61*, 6640–6648.

Burd, C.G., Strochlic, T.I., and Gangi Setty, S.R. (2004). Arf-like GTPases: Not so Arf-like after all. Trends Cell Biol. *14*, 687–694.

Calin, G.A., Cimmino, A., Fabbri, M., Ferracin, M., Wojcik, S.E., Shimizu, M., Taccioli, C., Zanesi, N., Garzon, R., Aqeilan, R.I., et al. (2008). MiR-15a and miR-16-1 cluster functions in human leukemia. Proc. Natl. Acad. Sci. USA *105*, 5166–5171.

Calin, G.A., Dumitru, C.D., Shimizu, M., Bichi, R., Zupo, S., Noch, E., Aldler, H., Rattan, S., Keating, M., Rai, K., et al. (2002). Frequent deletions and down-regulation of micro- RNA genes miR15 and miR16 at 13q14 in chronic lymphocytic leukemia. Proc. Natl. Acad. Sci. USA *99*, 15524–15529.

Calin, G.A., Ferracin, M., Cimmino, A., Di Leva, G., Shimizu, M., Wojcik, S.E., Iorio, M.V., Visone, R., Sever, N.I., Fabbri, M., et al. (2005). A MicroRNA signature associated with prognosis and progression in chronic lymphocytic leukemia. N. Engl. J. Med. *353*, 1793–1801.

Chiorazzi, N., and Ferrarini, M. (2003). B cell chronic lymphocytic leukemia: Lessons learned from studies of the B cell antigen receptor. Annu. Rev. Immunol. *21*, 841–894.

Cigudosa, J.C., Rao, P.H., Calasanz, M.J., Odero, M.D., Michaeli, J., Jhanwar, S.C., and Chaganti, R.S. (1998). Characterization of nonrandom chromosomal gains and losses in multiple myeloma by comparative genomic hybridization. Blood *91*, 3007–3010.

Cimmino, A., Calin, G.A., Fabbri, M., Iorio, M.V., Ferracin, M., Shimizu, M., Wojcik, S.E., Aqeilan, R.I., Zupo, S., Dono, M., et al. (2005). miR-15 and miR-16 induce apoptosis by targeting BCL2. Proc. Natl. Acad. Sci. USA *102*, 13944–13949.

Corcoran, M.M., Rasool, O., Liu, Y., Iyengar, A., Grander, D., Ibbotson, R.E., Merup, M., Wu, X., Brodyansky, V., Gardiner, A.C., et al. (1998). Detailed molecular delineation of 13q14.3 loss in B-cell chronic lymphocytic leukemia. Blood *91*, 1382–1390.

Damle, R.N., Wasil, T., Fais, F., Ghiotto, F., Valetto, A., Allen, S.L., Buchbinder, A., Budman, D., Dittmar, K., Kolitz, J., et al. (1999). Ig V gene mutation status and CD38 expression as novel prognostic indicators in chronic lymphocytic leukemia. Blood *94*, 1840–1847.

Döhner, H., Stilgenbauer, S., Benner, A., Leupolt, E., Krober, A., Bullinger, L., Döhner, K., Bentz, M., and Lichter, P. (2000). Genomic aberrations and survival in chronic lymphocytic leukemia. N. Engl. J. Med. *343*, 1910–1916.

Fulci, V., Chiaretti, S., Goldoni, M., Azzalin, G., Carucci, N., Tavolaro, S., Castellano, L., Magrelli, A., Citarella, F., Messina, M., et al. (2007). Quantitative technologies establish a novel microRNA profile of chronic lymphocytic leukemia. Blood *109*, 4944–4951.

Fürstenberger, G., and Senn, H.J. (2002). Insulin-like growth factors and cancer. Lancet Oncol. *3*, 298–302.

Gaidano, G., Ballerini, P., Gong, J.Z., Inghirami, G., Neri, A., Newcomb, E.W., Magrath, I.T., Knowles, D.M., and Dalla-Favera, R. (1991). p53 mutations in human lymphoid malignancies: Association with Burkitt lymphoma and chronic lymphocytic leukemia. Proc. Natl. Acad. Sci. USA *88*, 5413–5417.

Ghia, P., Chiorazzi, N., and Stamatopoulos, K. (2008). Microenvironmental influences in chronic lymphocytic leukaemia: The role of antigen stimulation. J. Intern. Med. *264*, 549–562.

Hamblin, T.J., Davis, Z., Gardiner, A., Oscier, D.G., and Stevenson, F.K. (1999). Unmutated Ig V(H) genes are associated with a more aggressive form of chronic lymphocytic leukemia. Blood *94*, 1848–1854.

Ivanov, D.V., Tyazhelova, T.V., Lemonnier, L., Kononenko, N., Pestova, A.A., Nikitin, E.A., Prevarskaya, N., Skryma, R., Panchin, Y.V., Yankovsky, N.K., et al. (2003). A new human gene KCNRG encoding potassium channel regulating protein is a cancer suppressor gene candidate located in 13q14.3. FEBS Lett. *539*, 156–160.

Kalachikov, S., Migliazza, A., Cayanis, E., Fracchiolla, N.S., Bonaldo, M.F., Lawton, L., Jelenc, P., Ye, X., Qu, X., Chien, M., et al. (1997). Cloning and gene mapping of the chromosome 13q14 region deleted in chronic lymphocytic leukemia. Genomics *42*, 369–377.

Klein, U., Tu, Y., Stolovitzky, G.A., Mattioli, M., Cattoretti, G., Husson, H., Freedman, A., Inghirami, G., Cro, L., Baldini, L., et al. (2001). Gene expression profiling of B cell chronic lymphocytic leukemia reveals a homogeneous phenotype related to memory B cells. J. Exp. Med. *194*, 1625–1638.

Lagos-Quintana, M., Rauhut, R., Lendeckel, W., and Tuschl, T. (2001). Identification of novel genes coding for small expressed RNAs. Science *294*, 853–858.

Landgren, O., Albitar, M., Ma, W., Abbasi, F., Hayes, R.B., Ghia, P., Marti, G.E., and Caporaso, N.E. (2009). B-cell clones as early markers for chronic lymphocytic leukemia. N. Engl. J. Med. *360*, 659–667.

Linsley, P.S., Schelter, J., Burchard, J., Kibukawa, M., Martin, M.M., Bartz, S.R., Johnson, J.M., Cummins, J.M., Raymond, C.K., Dai, H., et al. (2007). Transcripts targeted by the microRNA-16 family cooperatively regulate cell cycle progression. Mol. Cell. Biol. *27*, 2240–2252.

Liu, Q., Fu, H., Sun, F., Zhang, H., Tie, Y., Zhu, J., Xing, R., Sun, Z., and Zheng, X. (2008). miR-16 family induces cell cycle arrest by regulating multiple cell cycle genes. Nucleic Acids Res. *36*, 5391–5404.

Liu, Y., Corcoran, M., Rasool, O., Ivanova, G., Ibbotson, R., Grander, D., Iyengar, A., Baranova, A., Kashuba, V., Merup, M., et al. (1997). Cloning of two candidate tumor suppressor genes within a 10 kb region on chromosome 13q14, frequently deleted in chronic lymphocytic leukemia. Oncogene *15*, 2463–2473.

Liu, Y., Hermanson, M., Grander, D., Merup, M., Wu, X., Heyman, M., Rasool, O., Juliusson, G., Gahrton, G., Detlofsson, R., et al. (1995). 13q deletions in lymphoid malignancies. Blood *86*, 1911–1915.

Mayr, C., Speicher, M.R., Kofler, D.M., Buhmann, R., Strehl, J., Busch, R., Hallek, M., and Wendtner, C.M. (2006). Chromosomal translocations are associated with poor prognosis in chronic lymphocytic leukemia. Blood *107*, 742–751.

Mertens, D., Wolf, S., Schroeter, P., Schaffner, C., Döhner, H., Stilgenbauer, S., and Lichter, P. (2002). Down-regulation of candidate tumor suppressor genes within chromosome band 13q14.3 is independent of the DNA methylation pattern in B-cell chronic lymphocytic leukemia. Blood *99*, 4116–4121.

Messmer, B.T., Albesiano, E., Efremov, D.G., Ghiotto, F., Allen, S.L., Kolitz, J., Foa, R., Damle, R.N., Fais, F., Messmer, D., et al. (2004). Multiple distinct sets of stereotyped antigen receptors indicate a role for antigen in promoting chronic lymphocytic leukemia. J. Exp. Med. *200*, 519–525.

Migliazza, A., Bosch, F., Komatsu, H., Cayanis, E., Martinotti, S., Toniato, E., Guccione, E., Qu, X., Chien, M., Murty, V.V., et al. (2001). Nucleotide sequence, transcription map, and mutation analysis of the 13q14 chromosomal region deleted in B-cell chronic lymphocytic leukemia. Blood *97*, 2098–2104.

Ponting, C.P., Oliver, P.L., and Reik, W. (2009). Evolution and functions of long noncoding RNAs. Cell *136*, 629–641.

Raveche, E.S., Salerno, E., Scaglione, B.J., Manohar, V., Abbasi, F., Lin, Y.C., Fredrickson, T., Landgraf, P., Ramachandra, S., Huppi, K., et al. (2007). Abnormal microRNA-16 locus with synteny to human 13q14 linked to CLL in NZB mice. Blood *109*, 5079–5086.

Rawstron, A.C., Bennett, F.L., O'Connor, S.J., Kwok, M., Fenton, J.A., Plummer, M., de Tute, R., Owen, R.G., Richards, S.J., Jack, A.S., et al. (2008). Monoclonal B-cell lymphocytosis and chronic lymphocytic leukemia. N. Engl. J. Med. *359*, 575–583.

Rondeau, G., Moreau, I., Bezieau, S., Petit, J.L., Heilig, R., Fernandez, S., Pennarun, E., Myers, J.S., Batzer, M.A., Moisan, J.P., et al. (2001). Comprehensive analysis of a large genomic sequence at the putative B-cell chronic lymphocytic leukaemia (B-CLL) tumour suppresser gene locus. Mutat. Res. *458*, 55–70.

Rosenwald, A., Ott, G., Krumdiek, A.K., Dreyling, M.H., Katzenberger, T., Kalla, J., Roth, S., Ott, M.M., and Müller-Hermelink, H.K. (1999). A biological role for deletions in chromosomal band 13q14 in mantle cell and peripheral t-cell lymphomas? Genes Chromosomes Cancer *26*, 210–214.

Stilgenbauer, S., Nickolenko, J., Wilhelm, J., Wolf, S., Weitz, S., Döhner, K., Boehm, T., Döhner, H., and Lichter, P. (1998). Expressed sequences as

candidates for a novel tumor suppressor gene at band 13q14 in B-cell chronic lymphocytic leukemia and mantle cell lymphoma. Oncogene *16*, 1891–1897.

Tobin, G., Thunberg, U., Karlsson, K., Murray, F., Laurell, A., Willander, K., Enblad, G., Merup, M., Vilpo, J., Juliusson, G., et al. (2004). Subsets with restricted immunoglobulin gene rearrangement features indicate a role for antigen selection in the development of chronic lymphocytic leukemia. Blood *104*, 2879–2885.

Weintraub, S.J., Prater, C.A., and Dean, D.C. (1992). Retinoblastoma protein switches the E2F site from positive to negative element. Nature *358*, 259–261.

Wendel-Hansen, V., Sallstrom, J., De Campos-Lima, P.O., Kjellstrom, G., Sandlund, A., Siegbahn, A., Carlsson, M., Nilsson, K., and Rosen, A. (1994). Epstein-Barr virus (EBV) can immortalize B-cll cells activated by cytokines. Leukemia *8*, 476–484.

Widhopf, G.F., 2nd, Rassenti, L.Z., Toy, T.L., Gribben, J.G., Wierda, W.G., and Kipps, T.J. (2004). Chronic lymphocytic leukemia B cells of more than 1% of patients express virtually identical immunoglobulins. Blood *104*, 2499–2504.

Yan, X.J., Albesiano, E., Zanesi, N., Yancopoulos, S., Sawyer, A., Romano, E., Petlickovski, A., Efremov, D.G., Croce, C.M., and Chiorazzi, N. (2006). B cell receptors in TCL1 transgenic mice resemble those of aggressive, treatment-resistant human chronic lymphocytic leukemia. Proc. Natl. Acad. Sci. USA *103*, 11713–11718.

Zhao, H., Kalota, A., Jin, S., and Gewirtz, A.M. (2009). The c-myb proto-oncogene and microRNA-15a comprise an active autoregulatory feedback loop in human hematopoietic cells. Blood *113*, 505–516.